CANCOM2024 – CANADIAN INTERNATIONAL CONFERENCE ON COMPOSITE MATERIALS

DEVELOPMENT AND IMPLEMENTATION OF A STRAIN RATE-DEPENDENT ELASTO-PLASTIC FAILURE MODEL FOR COMPOSITE MATERIALS

Rouf, Khizar[1], Koltzenburg, Nils[1,2], Worswick, Mike[1], and Montesano, John[1]*
[1]Mechanical and Mechatronics Engineering, University of Waterloo, Waterloo, Canada
[2]Institute of Engineering Mechanics, Karlsruhe Institute of Technology, Karlsruhe, Germany
*John Montesano (john.montesano@uwaterloo.ca)

Keywords: *Constitutive modelling, Strain rate dependency, Non-crimp fabric composites*

ABSTRACT

A constitutive model is developed for predicting the strain rate-dependent pre-peak non-linear response and failure of unidirectional fiber-reinforced plastics. The constitutive model is formulated based on the mathematical framework of invariant theory for anisotropic materials. Strain rate dependency is incorporated through logarithmic scaling functions for the elastic, yield and failure parameters. The constitutive equations are solved numerically by the backward Euler method, and a user defined subroutine is developed and implemented in LS-DYNA for shell elements. The model is calibrated and verified for a non-crimp fabric composite by simulating the single element response for the transverse tension, transverse compression, in-plane shear and out-of-plane shear at different strain rates. The model is found to capture the elastic response, inelastic response, failure initiation and strain rate-dependency with good accuracy. The model is validated for a $[\pm 45]_{2s}$ laminate of the same non-crimp fabric composite at the quasi-static and high strain rates. An excellent agreement was found between the predicted and experimental results.

1 INTRODUCTION

Fiber-reinforced plastics (FRPs) are increasingly considered for load-bearing automotive applications due to their high specific stiffness and strength and tailorable energy absorption. FRPs manufactured through high-pressure resin transfer molding (HP-RTM) with snap-cure epoxy (e.g., unidirectional non-crimp fabric (UD-NCF) composites) offer short production cycles and low cost, thus are considered suitable for the automotive industry [1]. The successful adoption of FRPs for structural applications requires computational tools that can simulate full-scale structural response accurately and efficiently. Virtual structural analysis is a cost-effective and efficient approach to predicting the impact performance of structures; however, the performance of a virtual structural analysis highly depends on the material models used for the simulations.

FRPs exhibit strong directional dependence in their deformation and failure response due to their anisotropic and heterogeneous nature. Sun and Chen [2] developed an orthotropic plasticity model to capture the pre-peak nonlinear response using a quadratic yield function that requires one parameter to calibrate the yield surface. The model was applied to boron/aluminum and AS/3501-5 composites, and an adequate agreement between the experimental and predicted results was found. Körber [3] applied that model to predict the strain rate-dependent response of the IM7/8552 composite. A good agreement between the predicted and experimental results was observed. Despite being a simple plasticity model that requires only one parameter to calibrate, the determination of that parameter requires testing several off-axis laminae and the model does not account for tension-compression asymmetry of the yield surface [3]. Goldberg et al. [4] developed and implemented a general quadratic 3D orthotropic yield function. A plane-stress version of that model was later developed and implemented by Tobias [5] to make the model suitable for shell elements. A good agreement was observed between the experimental and single element verification results at the lamina level. Similar to the one-parameter model, the model developed by Goldberg et al. [4] and later modified by Tobias [5] also requires additional testing such as testing laminae in off-axis directions for the proper calibration of the yield surface. Tan et al. [6] developed a strain rate-dependent micromechanically motivated deformation model based on the concept of crystal plasticity to capture shear deformation modes of unidirectional tape composites (UDTCs). The model was validated for several strain rate-dependent cases that include off-axis laminae and laminates, and a good agreement was observed. However, a small mesh size (less than 1 mm) is required to accurately predict the stress-strain response that makes this model unsuitable for component-level simulations. Vogler et al. [7] developed a 3D elasto-plastic model for composite materials following the mathematical framework of the invariant formulation for transversely isotropic materials [8]. An excellent agreement was observed between the experimental and predicted results. The model developed by Vogler et al. [7] was extended by Körber et al. [9] to incorporate the strain rate and viscoplastic effects. Aamir et al. [10] have also developed and implemented modified formulations of the 3D invariant-based elasto-plastic model to incorporate other behaviors.

Different approaches for predicting failure initiation have been attempted in the last decades. They include maximum stress [11] criteria, maximum strain [12] criteria, interactive criteria [13, 14], which do not distinguish between failure modes, and physically based criteria [15, 16, 17], which distinguish at least between matrix and fiber failure (FF). Matrix failure, also called inter-fiber failure (IFF), occurs due to fracture in planes perpendicular to planes with the fiber direction as their normal direction [18, 16]. IFF criteria based on a fracture plane concept as deployed by Puck [16] or Pinho et al. [17] require the determination of the potential fracture plane, which is not analytically possible for general stress states. Thus, numerical optimization is commonly used for the fracture plane search [19, 20], but the numerical effort is, in general, increased compared to the approach using invariants. Invariant-based failure criteria [21, 22] are computationally more efficient since they do not require angle search procedures and have been shown to predict the failure initiation with good accuracy. Existing invariant-based failure criteria require biaxial tension and compression tests or off-axis tests, which increase the experimental work, especially when the characterization must perform at different strain rates, or suffer from an undesirable effect of the tensile strength on the compressive failure predictions (and vice versa).

In the presented research work [23, 24], an invariant-based strain rate-dependent elasto-inelastic failure model was formulated for shell elements. A user-defined subroutine was developed and implemented in LS-DYNA. The subroutine was verified for the transverse tension and compression, longitudinal tension and compression, in-plane and out-of-plane shear modes and validated for a laminate at quasi-static and high strain rates.

2 CONSTITUTIVE MODEL DEVELOPMENT AND IMPLEMENTATION

The constitutive equations for the elastic-plastic response of FRPs are established by following the mathematical framework of the invariant formulation [25]. In the invariant formulation, anisotropic constitutive relations are represented by means of a set of irreducible invariants of the stress tensor. The invariant formulation for transversely isotropic materials utilizes a structural tensor as an argument for the constitutive equations, which reflects material symmetries [25]. The structural tensor ($\underline{A}$) is obtained by the dyadic product ($\otimes$) of the preferred (normalized) direction vector that depends on the anisotropic nature of the material.

2.1.1 *Elasticity*

The elastic free energy in terms of strain and the structural tensor for a transversely isotropic material is defined as [25]:

$$\psi(\underline{\varepsilon}, \underline{A}) = \frac{1}{2}\lambda(\mathrm{tr}\,\underline{\varepsilon})^2 + \mu_\mathrm{T}\mathrm{tr}(\underline{\varepsilon})^2 + \alpha(\mathrm{tr}\,\underline{A\varepsilon})\mathrm{tr}\,\underline{\varepsilon} + 2(\mu_\mathrm{L} - \mu_\mathrm{T})(\mathrm{tr}\,\underline{A\varepsilon^2}) + \frac{1}{2}\beta(\mathrm{tr}\,\underline{A\varepsilon})^2 \tag{1}$$

where $\underline{\varepsilon}$ and $\underline{\mathrm{A}} = \tilde{a} \otimes \tilde{a}$ represent the strain and the structural second order tensors, respectively, and λ, μ_T, μ_L, α and β are scalar coefficients. $\tilde{a}$ is the preferred direction (a unit vector along the fiber direction in this case).

Taking the first derivative of the elastic free energy with respect to the strain yields the stress as a function of the strain and structural tensor:

$$\underline{\sigma}(\underline{\varepsilon}, \underline{A}) = \lambda(\mathrm{tr}\,\underline{\varepsilon})\underline{I} + 2\mu_\mathrm{T}\underline{\varepsilon} + \alpha\left((\mathrm{tr}\,\underline{A\varepsilon})\underline{I} + (\mathrm{tr}\,\underline{\varepsilon})\underline{A}\right) + 2(\mu_\mathrm{L} - \mu_\mathrm{T})(\underline{A\varepsilon} + \underline{\varepsilon A}) + \beta(\mathrm{tr}\,\underline{A\varepsilon})\underline{A} \tag{2}$$

where $\underline{I}$ represents the second order identity tensor.

By taking the second derivative of the elastic free energy with respect to the strain, the elasticity tensor, $\mathbb{C}$, for a transversely isotropic material can be written in the form of invariants as:

$$\mathbb{C} = \lambda\underline{I}\otimes\underline{I} + 2\mu_\mathrm{T}\mathbb{I} + \alpha(\underline{A}\otimes\underline{I} + \underline{I}\otimes\underline{A}) + 2(\mu_\mathrm{L} - \mu_\mathrm{T})\mathbb{I}_{\boldsymbol{A}} + \beta\underline{A}\otimes\underline{A} \tag{3}$$

where $\mathbb{I}_{\boldsymbol{A}} = A_{im}\mathbb{I}_{jmkl} + A_{jm}\mathbb{I}_{mikl}$ and $\mathbb{I}$ is the fourth order identity tensor.

The stress-strain relationship, for the plane stress form, is formulated by enforcing $\sigma_{33} = 0$.

2.1.2 *Yielding*

The transversely isotropic yield function (Equation 4) considers the inelastic response in the in-plane transverse direction, in-plane shear, out-of-plane shear, tension-compression asymmetry and plastic inextensibility along the fiber direction. The yield function consists of three terms, and it reads as:

$$f_\mathrm{y} = \alpha_1 I_{\mathrm{y}1} + \alpha_2 I_{\mathrm{y}2} + \alpha_3 I_{\mathrm{y}3} \tag{4}$$

In Equation 4, stress invariants ($I_{\mathrm{y}1}$, $I_{\mathrm{y}2}$ and $I_{\mathrm{y}3}$) and the yield parameters (α_1, α_2, and α_3) represent three loading states; out-of-plane shear, in-plane shear and uniaxial transverse tension/compression. To capture the tension-compression asymmetry, a case distinction for α_3 based on transverse tension or compression is used. The yield function (Equation 4) does not consider biaxial loadings since they are only important in the high hydrostatic loadings [7] I_{y1}, I_{y2} and I_{y3} are defined as [25]:

$$I_{\mathrm{y}1} = \frac{1}{2}\mathrm{tr}\,(\underline{\sigma}^{\mathrm{pind}})^2 - \mathrm{tr}\,\underline{A}(\underline{\sigma}^{\mathrm{pind}})^2 \tag{5}$$

$$I_{\mathrm{y}2} = \mathrm{tr}\,\underline{A}(\underline{\sigma}^{\mathrm{pind}})^2 \tag{6}$$

$$I_{\mathrm{y}3} = \mathrm{tr}\,\underline{\sigma} - \mathrm{tr}\,\underline{A\sigma} \tag{7}$$

$\underline{\sigma}^{\mathrm{pind}}$ is obtained by the following additive decomposition of the stress tensor:

$$\sigma^{\mathrm{r}} = \frac{1}{2}(\mathrm{tr}\,\sigma - \mathrm{tr}\,A\sigma)\underline{I} - \frac{1}{2}(\mathrm{tr}\,\sigma - 3\mathrm{tr}\,A\sigma)\underline{A} \tag{8}$$

$$\sigma^{\mathrm{pind}} = \sigma - \sigma^{\mathrm{r}} \tag{9}$$

2.1.3 Failure

Three failure modes are considered for capturing the failure initiation that include i) fiber failure in tension, ii) fiber failure in compression, and iii) matrix failure (IFF). Fiber failure in tension and compression is captured by applying the maximum stress criteria [11] and fiber kinking model [22], respectively. A new invariant-based criteria is developed for the predicting the IFF. The model is developed such that it does not require any off-axis or biaxial testing for calibration. The failure function for IFF reads as:

$$f_{\mathrm{IFF}} = \gamma_1 I_{\mathrm{f1}} + \gamma_2 I_{\mathrm{f2}} + \gamma_4 I_{\mathrm{f4}} \tag{10}$$

In Equation 10, γ_1, γ_2 and γ_3 are the failure parameters, which utilize the same case distinction for γ_1 as for α_3, while I_{f1}, I_{f2} and I_{f3} are three stress invariants that are defined as:

$$I_{\mathrm{f1}} = I_{\mathrm{y3}} = \mathrm{tr}\,\underline{\sigma} - \mathrm{tr}\,\underline{A\sigma} \tag{11}$$

$$I_{\mathrm{f2}} = I_{\mathrm{y2}} = \mathrm{tr}\,\underline{A}\left(\underline{\sigma}^{\mathrm{pind}}\right)^2 \tag{12}$$

$$I_{\mathrm{f4}} = 4I_{\mathrm{y1}} = 2\mathrm{tr}\left(\underline{\sigma}^{\mathrm{pind}}\right)^2 - 4\mathrm{tr}\,\underline{A}\left(\underline{\sigma}^{\mathrm{pind}}\right)^2 \tag{13}$$

Strain rate dependency for both the yield function and failure model is incorporated by applying a logarithmic scaling function. Further details about the model development and parameter identification can be found in [23, 24].

2.1.4 Implementation

For the sake of brevity, the governing equations in the numerical discretized form are not shown here, but the reader is referred to [23]. The constitutive equations of the material model are solved numerically by discretizing in time at Gauss-point level within FE framework. Time integration is performed using the backward Euler integration scheme. A user defined material model is developed in FORTRAN based on the numerical solution of the constitutive equations and implemented in LS-DYNA (Explicit) for the verification of the material model.

3 RESULTS AND DISCUSSION

The material model is calibrated using strain rate-dependent experimental data that was obtained through the experimental characterization of the UD-NCF composite material in our previous work [26]. Figure 1 presents the failure and yield surfaces in the $\sigma_{22} - \sigma_{12}$ space and failure surfaces in the $\sigma_{11} - \sigma_{12}$ and $\sigma_{11} - \sigma_{22}$ spaces. The yield surfaces for the $\sigma_{11} - \sigma_{12}$ and $\sigma_{11} - \sigma_{22}$ spaces are not shown since the yield function does not contain σ_{11} term due to the fiber inextensibility (i.e., the resulting envelope will be straight lines in the $\sigma_{11} - \sigma_{12}$ and $\sigma_{11} - \sigma_{22}$ spaces). All uniaxial strengths are met that verifies the correct calibration of the material model. The model captures the increase in the yield strength and failure strength with the increase in strain rate, except for the transverse tension mode for the yielding and longitudinal tension for the failure since both of these modes do not exhibit strain rate dependency [26], and the corresponding measures are strain rate-independent.

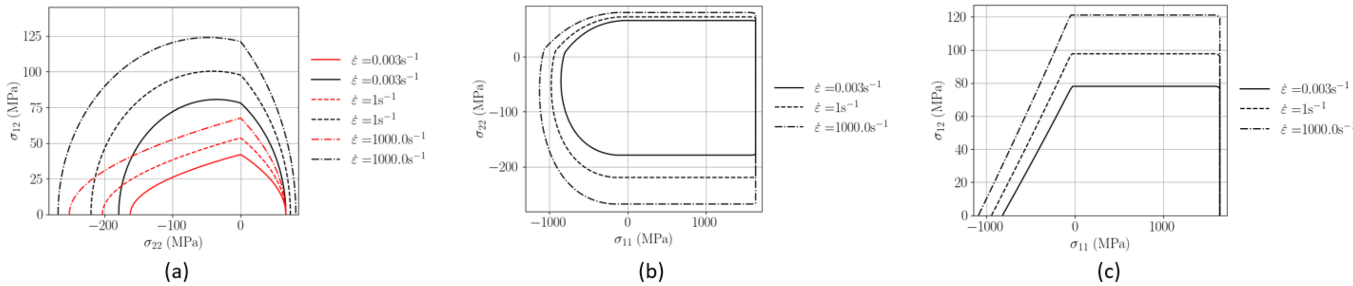

Figure 1: (a) Failure (in black color) and yield (in red color) surface in $\sigma_{22} - \sigma_{12}$ space, (b) Failure surface in $\sigma_{11} - \sigma_{12}$ space, (b) Failure surface in $\sigma_{11} - \sigma_{22}$ space

The material model was also validated at the single element level by subjecting the laminate of $[\pm 45]_{2s}$ stacking sequence to the axial compression loading conditions at the quasi-static and high-rate loading. The model predicted the elastic-inelastic and failure response with very good accuracy at both the quasi-static and high rate. Currently, the model is being further being tested for other laminates and incorporating post-peak damage.

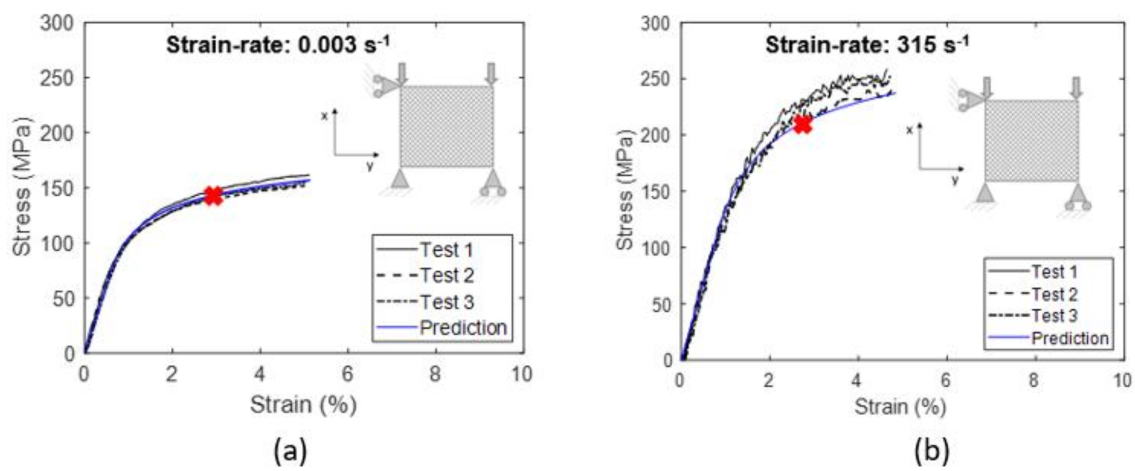

Figure 2: A comparison of the experimental and predicted test results of the [±45]2s laminate at: (a) Quasi-static strain rate, (b) High strain rate (The red mark on the plots indicates the failure initiation)

4 Conclusion

A strain rate-dependent invariant-based constitutive model is developed for shell elements and implemented in LS-DYNA for predicting the strain rate-dependent elastic-inelastic deformation and failure response of unidirectional fiber-reinforced plastics. The model is calibrated and verified for a UD-NCF composite material by simulating the single element response for the transverse tension and compression, longitudinal tension and compression, and in-plane shear mode at different strain rates. The first step validation is also achieved for the $[\pm 45]_{2s}$ laminate under uniaxial compression loading at quasi-static and high strain rates. The predicted results compare well with the experimental ones. In future, the model will be validated for other laminates and other features (post-peak damage and constraining effects) will be incorporated in the model.

5 REFERENCES

[1] A. Cherniaev, Y. Zeng, D. Cronin and J. Montesano, "Quasi-static and dynamic characterization of unidirectional non-crimp carbon fiber fabric composites processed by HP-RTM.," *Polymer Testing,* pp. 365-375, 2019.

[2] C. T. Sun and J. L. Chen, "A simple flow rule for characterizing nonlinear behavior of fiber composites.," *Journal of Composite Materials,* vol. 23, no. 10, pp. 1009-1020, 1989.

[3] H. Körber, "Mechanical response of advanced composites under high strain rates.," PhD dissertation, University of Porto, 2010.

[4] R. K. Goldberg, K. S. Carney, P. DuBois, C. Hoffarth, J. Harrington, S. Rajan and G. Blankenhorn, "Development of an orthotropic elasto-plastic generalized composite material model suitable for impact problems.," *Journal of Aerospace Engineering,* vol. 29, no. 4, p. 04015083, 2016.

[5] T. Achstetter, "Development of a composite shell-element model for impact applications.," Doctoral dissertation, George Mason University, 2019.

[6] W. Tan and B. Liu, "A physically-based constitutive model for the shear-dominated response and strain rate effect of Carbon Fibre Reinforced composites.," *Composites Part B: Engineering,* vol. 193, p. 108032, 2020.

[7] M. Vogler, G. Ernst and R. Rolfes, "Invariant based transversely-isotropic material and failure model for fiber-reinforced polymers.," *Computers, Materials, & Continua,* vol. 16, no. 1, pp. 25-50, 2010.

[8] Q. S. Zheng and A. J. M. Spencer, "Tensors which characterize anisotropies," *International Journal of Engineering Science,* vol. 31, no. 5, pp. 679-693, 1993.

[9] H. Koerber, P. Kuhn, M. Ploeckl, F. Otero, P. W. Gerbaud, R. Rolfes and P. P. Camanho, "Experimental characterization and constitutive modeling of the non-linear stress–strain behavior of unidirectional carbon–epoxy under high strain rate loading," *Advanced Modeling and Simulation in Engineering Sciences,* vol. 5, no. 1, pp. 1-24, 2018.

[10] A. Dean, J. Reinoso, S. Sahraee, B. Daum and R. Rolfes, "Invariant-based finite strain anisotropic material model for fiber-reinforced composites.," *Multiscale Modeling of Heterogeneous Structures,* pp. 83-110, 2018.

[11] P. A. Zinoviev, S. V. Grigoriev, O. V. Lebedeva and L. P. Tairova, "The strength of multilayered composites under a plane-stress state.," *Composites Science and Technology,* vol. 58, no. 7, pp. 1209-1223, 1998.

[12] T. A. Bogetti, C. P. Hoppel, V. M. Harik, J. F. Newill and B. P. Burns, "Predicting the nonlinear response and progressive failure of composite laminates.," in *In Failure criteria in fibre-reinforced-polymer composites*, Elsevier, 2004, pp. 402-428.

[13] S. W. Tsai and E. M. Wu, "A general theory of strength for anisotropic materials.," *Journal of composite materials,* vol. 5, no. 1, pp. 58-80, 1971.

[14] I. M. Daniel, S. M. Daniel and J. S. Fenner, "A new yield and failure theory for composite materials under static and dynamic loading.," *International Journal of Solids and Structures,* vol. 148, pp. 79-93, 2018.

[15] Z. Hashin, " Journal of Applied Mechanics," *Fatigue failure criteria for unidirectional fiber composites. ,* vol. 47, no. 4, pp. 329-334, 1980.

[16] A. Puck, Festigkeitsanalyse von faser-matrix-laminaten: modelle für die Praxis., Hanser., 1996.

[17] S. T. Pinho, R. Darvizeh, P. S. C. Robinson and P. P. Camanho, "Material and structural response of polymer-matrix fibre-reinforced composites.," *Journal of Composite Materials, 46(19-20), 2313-2341.,* vol. 46, no. 19, pp. 2313-2341, 2012.

[18] J. Hund, C. Leppin, T. Böhlke and J. Rothe, "Stress-strain characterization and damage modeling of glass-fiber-reinforced polymer composites with vinylester matrix.," *Journal of Composite Materials,* vol. 51, no. 4, pp. 547-562, 2017 .

[19] A. Puck and H. Schürmann, "Failure analysis of FRP laminates by means of physically based phenomenological models.," *Composites Science and Technology,* vol. 58, p. 1045–1067, 1998.

[20] J. Wiegand, N. Petrinic and B. Elliott, "An algorithm for determination of the fracture angle for the three-dimensional Puck matrix failure criterion for UD composites.," *Composites Science and Technology,* vol. 68, no. 12, pp. 2511-2517, 2008.

[21] R. M. Christensen, The theory of materials failure., Oxford University Press, USA., 2013.

[22] P. P. Camanho, A. Arteiro, A. R. Melro, G. Catalanotti and M. Vogler, "Three-dimensional invariant-based failure criteria for fibre-reinforced composites.," *International Journal of Solids and Structures,* vol. 55, pp. 92-107, 2015.

[23] K. Rouf, M. Worswick and J. Montesano, "An invariant-based strain rate-dependent inelastic deformation model for composite materials: Shell-Element Formulation and Finite Element Implementation.," *In-review.*

[24] N. Koltzenburg, K. Rouf, T. B¨ohlke and J. Montesano, "Development and experimental validation of a strain rate-dependent failure criteria for unidirectional noncrimp fabric composites.," *In-review.*

[25] J. Boehler, Applications of tensor functions in solid mechanics., Vienna: Springer, 1987.

[26] K. Rouf, M. Worswick and J. Montesano, "Effect of strain rate on the in-plane orthotropic constitutive response and failure behaviour of a unidirectional non-crimp fabric composite.," *Composites Part A: Applied Science and Manufacturing,* vol. 181, p. 108166, 2024.